*Geophys. J. R. astr. Soc.* (1982) 71, 151–158

# Inefficient propagation of $S_n$ under south-eastern China

Stuart Wier *Cooperative Institute for Research in Environmental Sciences (CIRES), University of Colorado/NOAA, Boulder, Colorado 80309, USA*

Received 1982 February 26; in original form 1980 May 27

**Summary.** Records of 21 earthquakes with ray paths crossing south-eastern China have been examined to establish the nature of propagation of the seismic wave $S_n$. $S_n$ is seen at stations within 1500 km of earthquakes, but not beyond 1500 km. No single localized region of attenuation can account for all the missing or weak $S_n$ waves. The inefficient propagation of $S_n$ through south-eastern China is surprising in light of efficient $S_n$ propagation in other continental platforms which, like south-eastern China, appear to have been stable throughout the Cenozoic.

## Introduction

$S_n$ is a seismic shear wave which propagates in the high-velocity mantle below the crust and above low-velocity zones. Having frequencies of 1–2 Hz or more, it is often seen on records from short-period instruments out to distances as large as 35° from the epicentre. $S_n$ usually initiates a wavetrain lasting several minutes, and the impulsive onsets may be used to calculate the velocity along the surface. Velocities near 4.7 km $s^{-1}$ are typical both for stable continental regions and old ocean basins (Huestis, Molnar, & Oliver 1973). $S_n$ velocities may be as low as 4.2 km $s^{-1}$ in some continents (Kadinsky-Cade *et al.* 1981).

Efficient propagation is characteristic of $S_n$ for much of the Earth's surface, especially shields, stable continental patforms, and ocean basins (Bath 1966; Molnar & Oliver 1969; Hart & Press 1973; Huestis *et al.* 1973). $S_n$ is severely attenuated by travel through the mantle under oceanic ridges, the concave sides of island arcs, and regions of Alpine mountain folding, such as the Himalayas and central Andes (Molnar & Oliver 1969; Barazangi *et al.* 1974; Chinn, Isacks & Barazangi 1980). Inefficient propagation is also found for the western United States, and part of the high plateaus of Turkey and Iran (Molnar & Oliver 1969; Kadinsky-Cade *et al.* 1981). The inefficient propagation of $S_n$ in these regions is though to be due to attenuation in the mantle, associated with a thin or absent lithospheric mantle lid between the crust and asthenosphere.

Where $S_n$ observed, its velocity is a direct measure of the shear velocity in the upper mantle immediately under the crust. In connection with a study of surface wave dispersion in China east of Tibet (Wier 1982), we decided to measure $S_n$ velocities in the same region to provide a constraint on the shear velocity structure of the uppermost mantle.

## Data analysis and results

Data from short-period seismographs at three World Wide Standard Seismograph Network stations adjacent to China were used in this study. The appearance of $S_n$ was checked on the horizontal component closest to transverse alignment with the ray path, and $P$ was measured on the vertical component. Earthquakes from 1963 to 1977 were considered for study, in an area from 20° to 40°N and from 98° to 125°E. Twenty-one earthquakes were well recorded and gave useful data. Their source data are listed in Table 1. All epicentral data and body-wave magnitudes are from the *Bulletin of the International Seismological Centre;* surface wave magnitudes are from the National Earthquake Information Service, United States Geological Survey. Locations of epicentres and seismograph stations are shown in Fig. 1. A few other earthquakes produced usable records at one of the three stations, showing $S_n$ propagation consistent with the result given here. All of the earthquakes had hypocentres in the crust. Most of the events used have magnitude $m_b$ 5.5 or more. Low magnifications (6250 or 12 500) of the short-period instruments at HKC and ANP precluded the routine use of smaller events.

This paper evaluates the quality of $S_n$ arrivals by the convention of Molnar & Oliver (1969), who ranked the appearance of $S_n$ waves by quality factors 0–3. Quality factor 2 corresponds to a clear arrival, amplitude at least one-half of the $P$-wave amplitude, and a predominate period between 1 and 1½ s. Quality factor 3 indicates an even larger wave with higher frequencies. $S_n$ waves of quality 2 or 3 are taken as indications of efficient propagation. Quality factors of 0 or 1 indicate absence of $S_n$ or very inefficient propagation. There is usually a clear distinction between ratings 1 and 2.

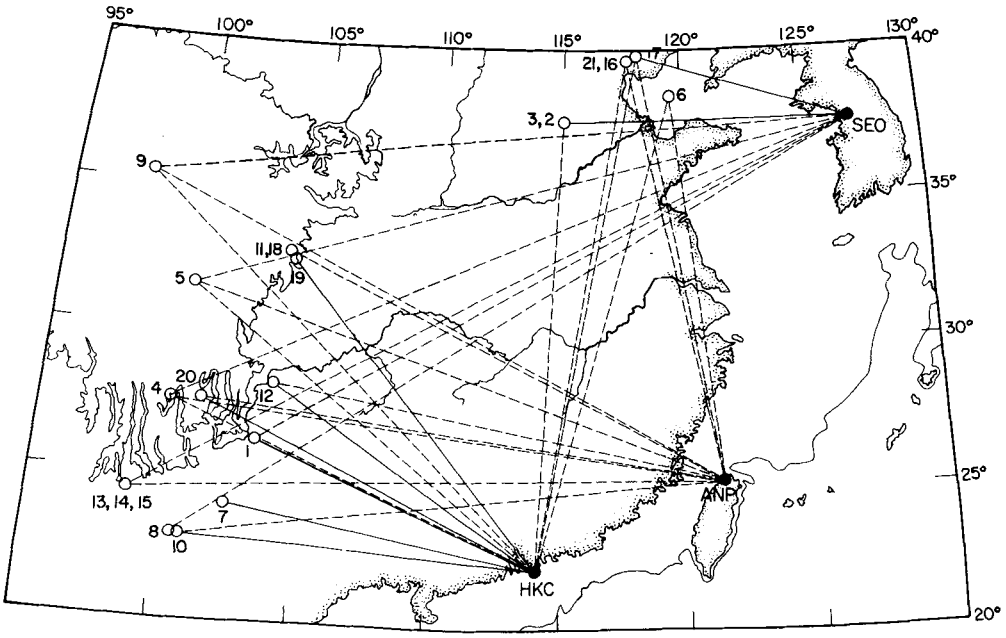


**Figure 1.** A map of the study area, showing the coastline of China, the 200 m contour below sea-level, the 2000 m contour above sea-level, seismograph station locations (solid circles), earthquake epicentres (open circles), paths of efficient $S_n$ propagation (solid lines), and paths of inefficient $S_n$ propagation (dashed lines).

**Table 1.** Source data for earthquakes used in this study.

| No. | Date | Origin time (hr min s) | Latitude (°N) | Longitude (°E) | Depth (km) | $m_b$ | $M_s$ |
|---|---|---|---|---|---|---|---|
| 1 | 1966 Feb. 5 | 15:12:32.9 | 26.22 | 103.21 | 32 | 5.6 | |
| 2 | 1966 Mar. 22 | 8:11:33.5 | 37.54 | 115.00 | 3 | 5.6 | |
| 3 | 1966 Mar. 29 | 6:12:08 | 37.52 | 114.99 | 33 | 5.3 | |
| 4 | 1966 Sep. 28 | 14:00:21 ± 2.5 | 27.53 | 100.08 | 12 | 5.7 | |
| 5 | 1967 Aug. 30 | 4:22:5.1 | 31.61 | 100.26 | 24 | 6.1 | |
| 6 | 1969 July 18 | 5:24:45 ± 2.1 | 38.43 | 119.47 | 6 | 5.9 | |
| 7 | 1970 Jan. 4 | 17:00:39.4 | 24.12 | 102.49 | 15 | 5.8 | 7.5 |
| 8 | 1970 Feb. 6 | 22:10:42.4 | 23.02 | 100.76 | 30 | 5.4 | 6.1 |
| 9 | 1971 Mar. 24 | 13:54:18.4 | 35.46 | 98.04 | 13 | 5.7 | 6.4 |
| 10 | 1971 Apr. 28 | 15:32:0.1 ± 3.0 | 22.98 | 101.02 | 11 | 5.6 | 6.3 |
| 11 | 1973 Aug. 11 | 7:15:38.2 | 32.94 | 104.02 | 20 | 5.5 | 6.1 |
| 12 | 1974 May 10 | 19:25:17 ± 1.2 | 28.19 | 103.98 | 17 | 5.8 | 6.8 |
| 13 | 1976 May 29 | 12:23:18.4 | 24.51 | 98.95 | 3 | 5.9 | 6.9 |
| 14 | 1976 May 29 | 14:00:19.4 | 24.54 | 98.60 | 4 | 5.7 | 7.0 |
| 15 | 1976 July 21 | 15:10:45.1 | 24.78 | 98.68 | 4 | 5.7 | 6.3 |
| 16 | 1976 July 27 | 19:42:54 ± 1.6 | 39.56 | 117.87 | 10 | 6.1 | 7.9 |
| 17 | 1976 July 28 | 10:45:37.2 | 39.71 | 118.37 | 37 | 6.1 | 7.4 |
| 18 | 1976 Aug. 16 | 14:06:45 ± 1.7 | 32.78 | 104.09 | 9 | 6.1 | 6.9 |
| 19 | 1976 Aug. 21 | 21:49:52 ± 1.7 | 32.59 | 104.24 | 15 | 6.0 | 6.4 |
| 20 | 1976 Nov. 6 | 18:04:06 ± 2.3 | 27.66 | 101.04 | 5 | 5.7 | 6.5 |
| 21 | 1976 Nov. 15 | 13:53:2.6 | 39.50 | 117.73 | 27 | 6.0 | 6.3 |

Many of the seismograms of waves crossing south-eastern China showed absent or weak $S_n$ waves. Fig. 1 shows that the ray paths associated with inefficient $S_n$ propagation cover much of south-eastern China. Fig. 2 shows several of the seismograms which lack $S_n$. A few earthquakes, within 1500 km of a recording station, produced seismograms with clear $S_n$.

A rating of 2 was assigned by Molnar & Oliver to the $S_n$ wave recorded at Seoul Korea (SEO) from the event of 1966 March 29 (no. 3, Table 2). A rating of 3 is assigned in this study to the $S_n$ wave from event no. 2, which has nearly the same epicentre as event no. 3, recorded at SEO. These events are only 9.5° (1058 km) from Seoul, and reception of clear $S_n$ is not remarkable considering the short distance between the earthquake and seismograph. Peak magnification at Seoul is 50 000. No impulsive onset is recorded for either of these waves, preventing a velocity estimate. A large, high-frequency signal is also seen at $S_n$ time at Seoul for the very powerful event no. 17, 7.1° (785 km) from Seoul.

All other earthquake recordings at SEO and ANP indicated that $S_n$ was absent or weak, receiving ratings of 0 or 1. All the earthquakes showing absent or weak $S_n$ at ANP and SEO were over 1500 km from the stations. The only exception is the record of event no. 6, 1482 km from ANP, which shows $S_n$ (rating 1) at ANP. Many events recorded at HKC showed the same phenomena.

Eight earthquakes recorded at HKC (nos 1, 7, 8, 10, 11, 12, 19 and 20) had $S_n$ waves of rating 2 or 3, indicating good $S_n$ propagation. All these events are located less than 1500 km from HKC, except no. 11 (1545 km) and no. 19 (1503 km). Fig. 3 shows seismograms from HKC which contain a wave at $S_n$ time. Other earthquakes recorded at HKC show weak or absent $S_n$, and are located over 1500 km from the station. An instructive comparison involves the records from no. 4 (1535 km; no sign of $S_n$) and event no. 20 (1451 km, $S_n$ rating 2). The ray paths to both events are very close.

Only one $S_n$ wave with an impulsive onset was found in this study; earthquake no. 19 recorded at HKC. If we assume an intercept time term of 10.0 s (Huestis *et al.* 1973), the

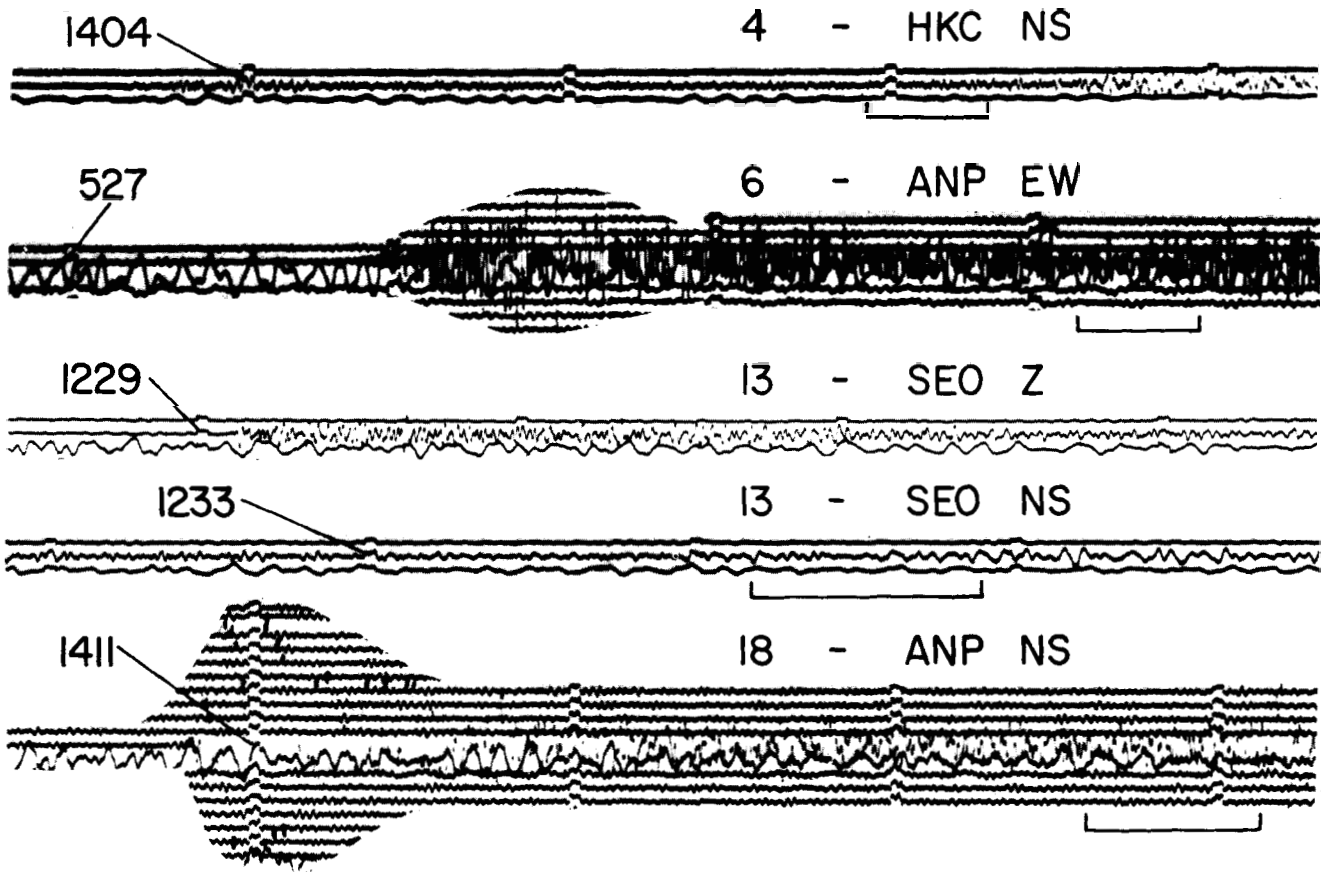


**Figure 2.** Examples of seismograms from this study showing weak or absent $S_n$ arrivals. Each seismogram is labelled with a time mark, an event number (from Table 1), the code of the receiving station and the component of ground motion. The bracket indicates an arrival time interval corresponding to velocities from 4.7 to 4.4 km $s^{-1}$. Vertical components are shown when the *P*-wave amplitude is poorly indicated by the horizontal record.

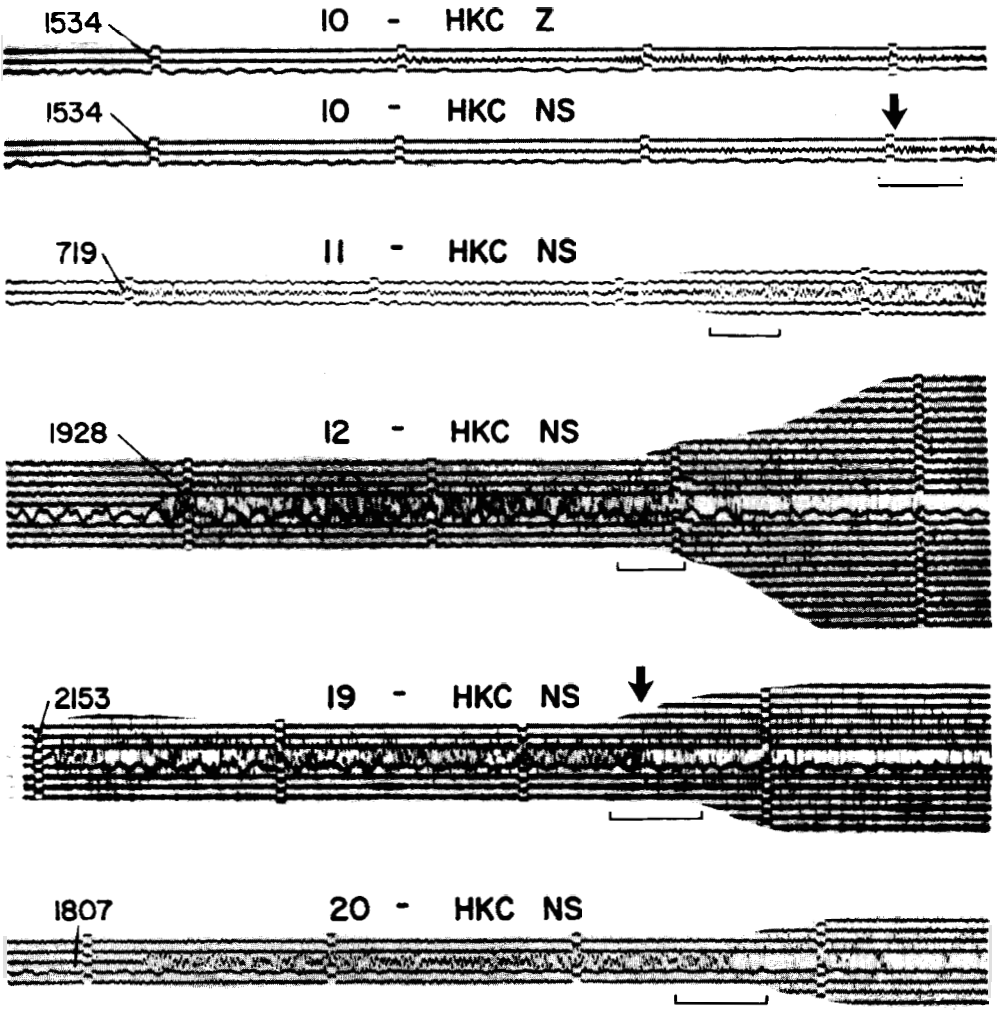


**Figure 3.** Examples of seismograms from this study showing good $S_n$ arrivals. Notation is the same as in Fig. 2. Vertical component of ground motion is shown for event 10 since it lies nearly due west of HKC and the *P*-wave amplitude is poorly indicated by the north–south component seismogram. Arrivals of $S_n$ from events 10 and 19 are shown by arrows.

observed travel time of 338.0 s, and include the standard error of origin time ±1.7 s, a velocity of $4.58 \pm 0.02\,\mathrm{km\,s^{-1}}$ is determined. Possible error in source depth determination, and crustal thickness variation, increase the uncertainty of this value. The $S_n$ wave from event 10 recorded at HKC is not impulsive but is clear enough to indicate an $S_n$ velocity near $4.60\,\mathrm{km\,s^{-1}}$ (Fig. 3). We are not justified in regarding these values as a definitive measure of $S_n$ velocity in south-eastern China since individual $S_n$ arrival times usually show large scatter (Kadinsky-Cade *et al.* 1981).

## Geological setting of south-eastern China

From a tectonic standpoint, south-eastern China may be defined as the part of China bordered by the Red River Fault, the Yunnan grabens between the Red River Fault and the

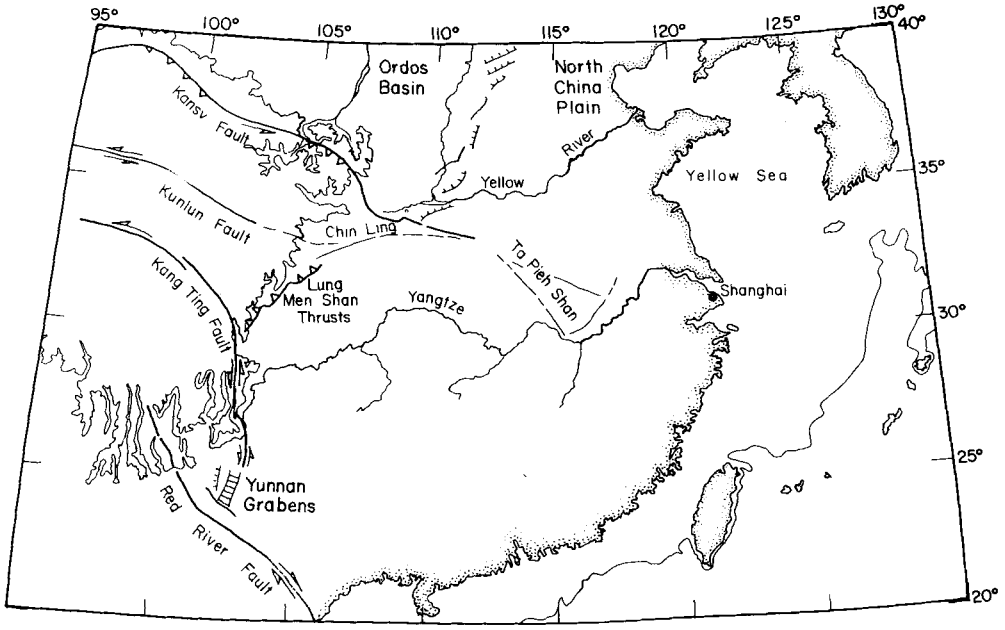


**Figure 4.** Sketch map of the study area showing the same geographical features as Fig. 1 and important faults (Terman 1973; Tapponnier & Molnar 1977).

Kang Ting Fault, the Kang Ting Fault, the Lung Men Shan Thrusts, the faults south of the Chin Ling mountains, the Ta Pieh Shan Foldbelt, and the Yangtze River between the Ta Pieh and Shanghai (Fig. 4; Tapponnier & Molnar 1977; Terman 1973). Little tectonic or volcanic activity has occurred in south-eastern China since the beginning of the Cenozoic, and in many places since the Palaeozoic (Tapponnier & Molnar 1977; Huang 1980). The youngest formations in the geological record in south-eastern China are Jurassic and Cretaceous volcanics and intrusives along the south-eastern coastal area (Terman 1973; Jahn 1974; Huang 1980). The geological structures of Korea appear to be continuous with those of eastern China (Wageman, Hilde & Emery 1970; Shi *et al.* 1975). The Yellow Sea is a shallow embayment covering the intervening continental platform.

Using satellite photographs and seismological data, as well as the available geological information, Tapponnier & Molnar (1977) have found that the faults mentioned above have been activated by the collision of the Indian plate with Eurasia. It is not known whether any other geological phenomena, such as enhanced heat flow, accompany the surface faulting phenomena which are often associated with the attenuation of $S_n$ waves. Tapponnier & Molnar refer to south-eastern China as the south-east China stable block and state that it appears to have been stable throughout the Cenozoic. Many of the seismic ray paths used in this study are largely confined to this stable continental block. The earthquake sources occur in the adjacent regions which are currently being faulted.

The paths to station SEO used in this study, and the paths from the epicentres near Peking, contain extensive portions outside south-eastern China as that area has been defined. Tapponnier & Molnar (1977) find evidence for recent extensional tectonics along the Ordos Basin's eastern limits and eastward through the North China Plain. Only limited evidence suggests recent tectonic movements between the Yellow River and the Yangtze east of 112°E (Tapponnier & Molnar 1977). It may be that this area is effectively part of the south-east China stable block, or it may be a transitional region between the stable block

south of the Yangtze and the active North China Plain north of the Yellow River. The historical earthquake record (York, Cardwell & Ni 1976) suggests the stable area may extend almost to the Yellow River and include the Yellow Sea and most of Korea. The only well-established recent volcanics of eastern China are the Hsing An basalts north of 41°N and basalts which outcrop locally in the grabens east of the Ordos Basin (Tapponnier & Molnar 1977; Simkin *et al.* 1981).

## Discussion

Several areas of the world are known to have poor $S_n$ propagation: ocean ridges, the concave side of island arcs, mountain belts of Alpide orogenies, the western United States, and parts of the high plateaus of Turkey and Iran. All of these have in common active geological deformation in the late Tertiary and Quaternary, extending up to the present. Several of these areas are known to be places where the mantle lithosphere is thin or missing. Recent volcanic activity is common in many of these areas.

The available geological data suggest that south-eastern China is a stable block which has been tectonically quiet throughout the Cenozoic. One expects $S_n$ to propagate efficiently through such a region. This study indicates weak $S_n$ waves are often recorded for paths crossing south-eastern China. This result is reminiscent of the suppression of high-frequency Lg waves in the same area (Ruzaikin *et al.* 1977). It may be that $S_n$ is attenuated in localized regions, such as under the North China Plain and under the mountains west of 105°E. Both of these areas are at present being deformed by active tectonic processes (Tapponnier & Molnar 1977). However, some $S_n$ waves are received at HKC from epicentres within the mountain ranges, and widespread rather than localized attenuation of $S_n$ in southeastern China is also a possible explanation of the observations.

The degree of attenuation of $S_n$ under China may depend on distance; $S_n$ is usually seen within 1500 km of an earthquake but rarely farther than 1500 km from an earthquake. The suggestion of a fairly abrupt cutoff at 1500 km is not perfectly established, but is similar to an abrupt suppression of $S_n$ beyond 1700 km in the Nazca plate (Chinn *et al.* 1980). Chinn *et al.* indicate that this is not consistent with the usual exponential attenuation of seismic waves with distance. $S_n$ propagation under China is more efficient than under mid-ocean ridges and parts of the plateaus of Iran and Turkey where a path segment only a few hundred kilometres in length is adequate to eliminate $S_n$ completely.

Where seen, the $S_n$ wave has a velocity near 4.60 km $s^{-1}$. This value is consistent with one earth model for south-eastern China determined from surface wave dispersion (Wier 1982). The model includes a thin (5 km) mantle 'lid' of 4.65 km $s^{-1}$ shear wave velocity, overlying a thick (180 km) low-velocity zone of 4.40 km $s^{-1}$ shear wave velocity. Such an earth model accounts both for the observed velocity of $S_n$ and its high degree of attenuation. The mantle lid permits $S_n$ propagation, but it will be more than usually attenuated due to the thinness of the lid and the adjacent low-velocity (and presumable low-$Q$) zone. An alternate explanation for inefficient $S_n$ propagation in south-eastern China involves the fact that the crust of south-eastern China is composed of several distinct geological provinces (Terman 1973; Huang 1980; McElhinney *et al.* 1981). Crustal thickness varies from over 50 km in the west to 30 km along the sea coast. Associated changes in upper mantle properties would create lateral variations in upper mantle seismic velocities, degrading the waveguide for $S_n$.

## Acknowledgments

We thank Douglas Chinn for his critical review of the manuscript. Seismograms were supplied by the Environmental Data Service, National Oceanic and Atmospheric Administration, Boulder, Colorado. Earthquake epicentre lists were prepared by Mr Wilbur

Rinehart of EDS. The research reported in this paper was performed at the Cooperative Institute for Research in Environmental Sciences (CIRES), Boulder, Colorado. CIRES is supported by the National Oceanic and Atmospheric Administration and the University of Colorado.

## References

Barazangi, M., Isacks, B., Dubois, J. & Pascal, G., 1974. Seismic wave attenuation in the upper mantle beneath the southwest Pacific, *Tectonophys.*, **24**, 1.

Bath, M., 1966. Propagation of $S_n$ and $P_n$ to teleseismic distances, *Pure appl. Geophys.*, **64**, 19.

Chinn, D., Isacks, B. & Barazangi, M., 1980. High frequency seismic wave propagation in western South America along the continental margin, in the Nazca plate, and across the Altiplano, *Geophys. J. R. astr. Soc.*, **60**, 209.

Hart, R. & Press, F., 1973. $S_n$ velocities and the composition of the lithosphere in the regionalized Atlantic, *J. geophys. Res.*, **78**, 407.

Huang, T., 1980. An outline of the tectonic characteristics of China, in *Continental Tectonics*, National Academy of Sciences, Washington.

Huestis, S., Molnar, P. & Oliver, J., 1973. Regional $S_n$ velocities and shear velocity in the upper mantle, *Bull seism. Soc. Am.*, **63**, 469.

Jahn, B., 1974. Mesozoic thermal events in southeast China, *Nature*, **248**, 480–483.

Kadinsky-Cade, K., Baranzangi, M., Oliver, J. & Isacks, B., 1981. Lateral variations of high-frequency seismic wave propagation at regional distances across the Turkish and Iranian Plateaus, *J. geophys. Res.*, **86**, 9377.

McElhinny, M., Embleton, B., Ma, X. & Zhang, Z., 1981. Fragmentation of Asia in the Permian, *Nature*, **293**, 212.

Molnar, P., & Oliver, J., 1960. Lateral variation of attenuation in the upper mantle and discontinuities in the lithosphere, *J. geophys. Res.*, **74**, 2648.

Ruzaikin, A., Nersesov, I., Khalturin, V. & Molnar, P., 1977. Propagation of Lg and lateral variations in crustal structure in Asia, *J. geophys. Res.*, **82**, 307.

Shi Zhen-liang, Huan, Wen-lin, Wu, Huang & Cao, Xin-ling, 1973. On the intensive seismic activity in China and its relation to plate tectonics (in Chinese), *Sci. Geol. Sinica*, **4**, 281 (translated by Chao, E. C. T., 1975. *Am. J. Sci.*, **275**, 239).

Simkin, T., Siebert, L., McClelland, L., Bridge, D., Newhall, C. & Latter, J., 1981. *Volcanoes of the World*, Hutchinson Ross, Stroudsburg.

Tapponnier, P. & Molnar, P., 1977. Active faulting and tectonics in China, *J. geophys. Res.*, **82**, 2905.

Terman, M. (principal compiler), 1973. *Tectonic Map of China and Mongolia*, (1:5,000,000), Geological Society of America.

Wageman, J., Hilde, T. & Emery, K., 1970. Structural framework of East China Sea and Yellow Sea, *Bull. Am. Ass. Petrol. Geol.*, **54**, 1611.

Wier, S., 1982. Surface wave dispersion and Earth structure in south-eastern China, *Geophys. J. R. astr. Soc.*, **69**, 33.

York, J., Cardwell, R. & Ni, J., 1976. Seismicity and quaternary faulting in China, *Bull. seism. Soc. Am.*, **66**, 1983.